Gas-Phase Chemistry

Efficient Room-Temperature Methane Activation by the Closed-Shell, Metal-Free Cluster [OSiOH]+: A Novel Mechanistic Variant

Xiaoyan Sun, Shaodong Zhou, Maria Schlangen, and Helmut Schwarz*[a]

Dedicated to Professor Jörn Müller, TU Berlin, on the occasion of his 80th birthday

Abstract: The closed-shell cluster ion [OSiOH]+ is generated in the gas phase and its reactivity towards the thermal activation of CH_4 has been examined using Fourier transform-ion cyclotron resonance (FT-ICR) mass spectrometry in conjunction with state-of-the-art quantum chemical calculations. Quite unexpectedly at room temperature, [OSiOH]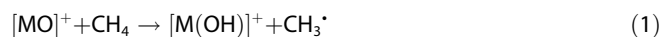+ efficiently mediates C—H bond activation, giving rise to [SiOH]+ and [SiOCH₃]+ with the concomitant formation of methanol and water, respectively. Mechanistic aspects for this unprecedented reactivity pattern are presented, and the properties of the [OSiOH]+/CH_4 couple are compared with those of the closed-shell systems [OCOH]+/CH_4 and [MgOH]+/CH_4; the last two couples exhibit an entirely different reactivity scenario.

Introduction

Selective activation of alkane C—H bonds constitutes a major challenge in the syntheses of value-added products. Methane, as the principal component of natural gas, is estimated as one of the largest hydrocarbon resources on earth, and activation of its thermodynamically stable and kinetically inert C—H bond under ambient conditions to produce transportable liquids as well as more valuable chemicals has been identified as one of the key challenges in the context of addressing the global energy problem.[1] Heterogeneous catalysis mediated by metal oxides, though rather inefficient, provides means to activate methane.[2] As demonstrated repeatedly, combined experimental/computational studies on the gas-phase reactions of metal-oxide clusters with methane have uncovered mechanistic aspects and shed light on the elementary steps of catalytic processes at a strictly molecular level, and may thus help to design new efficient catalysts.[3]

In previous studies, different types of methane activation by gaseous open-shell oxide cluster ions have been identified. The first variant involves hydrogen-atom transfer (HAT) to produce [M(OH)]+ with the liberation of CH_3 [Eq. (1)].[4] Here, the reactive species may correspond to simple diatomic oxides [MO]+ as well as to larger cluster oxides [M_xO_y]+ possessing a higher nuclearity, and it has been shown that a high spin density at a terminal oxygen atom is key to bring about efficient HAT.[4,5] Spin states also play a major role in the thermal

reactions of simple diatomic [MO]+ species, including, for example, [FeO]+, [CuO]+, and [AuO]+,[6] with methane to form CH_3OH [Eq. (2)]. For a proper understanding in this case, a two-state reactivity (TSR) scenario needs to be invoked, that is, in thermal reactions excited spin states are involved.[7] For those metal oxides or bare metals which, due to large relativistic effects,[8] afford very strong metal–carbon bonds, a third variant for activating methane is operative giving rise to metal–carbene formation[9] along with the expulsion of water [Eq. (3)]; typical examples include [PtO]+ and [OsO₂]+.[3d, 10]

$$[MO]^+ + CH_4 \rightarrow [M(OH)]^+ + CH_3^\bullet \tag{1}$$

$$[MO]^+ + CH_4 \rightarrow M^+ + CH_3OH \tag{2}$$

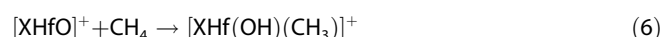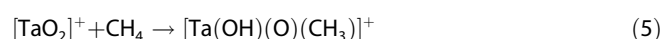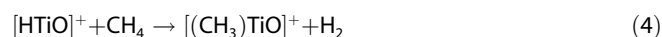$$[MO]^+ + CH_4 \rightarrow [M(CH_2)]^+ + H_2O \tag{3}$$

Recently, quite rare examples for the thermal reaction of methane mediated by closed-shell oxide clusters were reported. Not surprisingly, in the absence of a radical center, the activation processes followed entirely different mechanisms, which highly depend on the composition and structural properties of the metal clusters. For example, for the [HTiO]+/CH_4 couple, which lacks a radical site at the oxygen atom and for which the penalty to decouple the Ti═O bond is much too high, the system bypasses the classical HAT and prefers to engage in a metathesis-like ligand exchange process involving the hydride ligand [Eq. (4)].[11] Also, the closed-shell cluster [TaO₂]+ brings about C—H bond activation at ambient conditions [Eq. (5)]. Here, the presence of a 5d element causes a much higher reactivity as compared to the lighter congeners of the Group 5 metal dioxide cluster cations [MO₂]+ (M═V, Nb); the difference in reactivity is likely due to relativistic effects, which favors the formation of a strong Ta—C bond.[12] Yet another ex-

[a] Dr. X. Sun, Dr. S. Zhou, Dr. M. Schlangen, Prof. Dr. H. Schwarz
Institut für Chemie
Technische Universität Berlin
Straße des 17. Juni 135, 10623 Berlin (Germany)
E-mail: Helmut.Schwarz@tu-berlin.de

These are not the final page numbers! ↗↗

ample of methane activation by a closed-shell oxide cluster is given in Equation (6). In contrast to the inertness of diatomic $[HfO]^+$ towards methane, the closed-shell, halogenated oxide ions $[XHfO]^+$ (X = F, Cl, Br) activate the $H_3C—H$ bond and form the insertion products $[XHf(OH)(CH_3)]^+$. The presence of the halogen ligand strengthens the formation of a Hf—C bond and, at the same time, weakens the π(Hf—O) bond such that C—H bond activation of CH_4 can take place under ambient conditions.[13]

$$[HTiO]^+ + CH_4 \rightarrow [(CH_3)TiO]^+ + H_2 \qquad (4)$$

$$[TaO_2]^+ + CH_4 \rightarrow [Ta(OH)(O)(CH_3)]^+ \qquad (5)$$

$$[XHfO]^+ + CH_4 \rightarrow [XHf(OH)(CH_3)]^+ \qquad (6)$$

Silicon oxide constitutes an abundant substance on earth and serves as an important catalyst support widely used in many large-scale chemical transformations.[14] This material is usually considered to act as a catalytically innocent linker between the active metal oxide sites and the support.[15] For example, high catalytic activities have been observed when SiO_2 is used as a support for the activation of methane, such as in the selective oxidation of methane to formaldehyde,[16] or the direct conversion of methane to ethylene.[17] In recent years, the concept of catalytic functionalization of C—H bonds using metal-free catalysts have fascinated scientists and led to important conceptual breakthroughs with regard to various aspects of C—H bond activation.[18] Therefore, probing the reactivity of silicon oxide clusters may not only deepen the mechanistic understanding of C—H bond activation by silica-supported systems, but may also shed light on the active site of a metal-free catalyst. Here, we report our combined experimental/computational findings on the gas-phase reactivity of the silicon oxide cluster $[OSiOH]^+$ towards CH_4, and a detailed comparison with the closed-shell systems $[OCOH]^+/CH_4$ and $[MgOH]^+/CH_4$ is made.

Results and Discussion

The cluster ion $[OSiOH]^+$ (m/z: 61) was generated in the reaction of $[SiO_2]^+$ with water; see the Experimental and Computational Details section for further information. The Fourier transform-ion cyclotron resonance (FT-ICR) mass spectra of the reactions of mass-selected, thermalized $[OSiOH]^+$ ions with methane are reproduced in Figure 1; the reactivity of $[OSiOH]^+$ toward inert argon as well as background impurities have been included as a reference spectrum (Figure 1a). When $[OSiOH]^+$ is exposed to methane (Figure 1b), two ionic products, $[SiOH]^+$ (m/z: 45) and $[SiOCH_3]^+$ (m/z: 59) are formed with a branching ratio of 35 and 65%, Eqs. (7) and (8), respectively. The rate constant $k([OSiOH]^+/CH_4)$ is determined to be 1.64×10^{-10} $cm^3 s^{-1}$ molecule^{-1}, corresponding to an efficiency of 22%, relative to the collision rate.[19] Mechanistic insights are provided by labeling experiments: reacting $[OSiOH]^+$ with CD_4 gives rise to the corresponding deuterated $[SiOD]^+$ and $[SiOCD_3]^+$ ions; quite unexpectedly, $[SiOH]^+$ and sparse
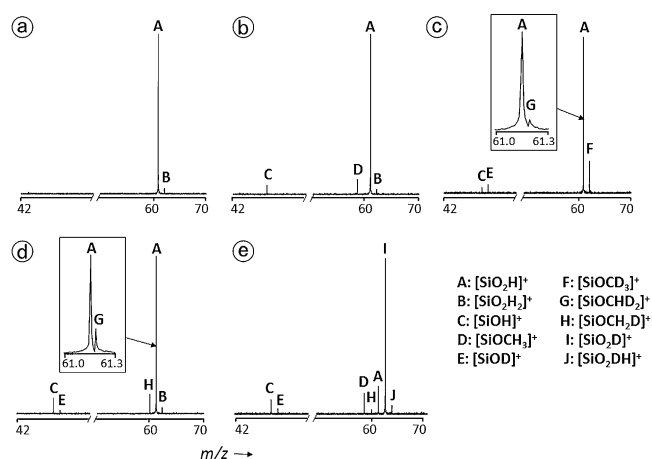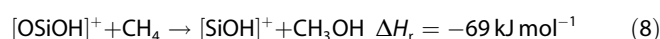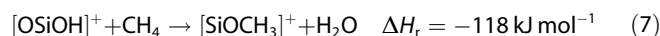

Figure 1. Mass spectra showing the room-temperature reactivity of $[OSiOH]^+$ with a) Ar, b) CH_4, c) CD_4, and d) CH_2D_2 at a pressure of 1.0×10^{-9} mbar and reaction delay of 15 s; and e) the reactivity of $[OSiOD]^+$ with CH_4 at a pressure of 2.0×10^{-9} mbar and reaction delay of 3 s. The signals labeled as **B** and **J** are due to the reaction with background impurities, and the signal **A** in e) is due to an H/D exchange between $[OSiOD]^+$ and background water.

A: $[SiO_2H]^+$ F: $[SiOCD_3]^+$
B: $[SiO_2H_2]^+$ G: $[SiOCHD_2]^+$
C: $[SiOH]^+$ H: $[SiOCH_2D]^+$
D: $[SiOCH_3]^+$ I: $[SiO_2D]^+$
E: $[SiOD]^+$ J: $[SiO_2DH]^+$

amounts of $[SiOCHD_2]^+$ are also observed. The ions $[SiOH]^+$:$[SiOD]^+$ are generated in a ratio of 1:1.8, while in the reaction with CH_2D_2, this ratio amounts to 4.2:1. We have also reacted $[OSiOD]^+$ with CH_4 (Figure 1e); here, the ratio $[SiOH]^+$:$[SiOD]^+$ amounts to 2.2:1. An interpretation of these branching ratios will be given below together with the analysis of the theoretical results. In the reactions of $[OSiOH]^+$ with CH_4 and CD_4, no intermolecular kinetic isotope effect (KIE) could be identified, that is, the intermolecular KIE is approximated to 1.0 within the error bars of the experiment.[20]

$$[OSiOH]^+ + CH_4 \rightarrow [SiOCH_3]^+ + H_2O \quad \Delta H_r = -118 \, kJ \, mol^{-1} \quad (7)$$

$$[OSiOH]^+ + CH_4 \rightarrow [SiOH]^+ + CH_3OH \quad \Delta H_r = -69 \, kJ \, mol^{-1} \quad (8)$$

Mechanistic insight into the details of the methane activation step by $[OSiOH]^+$ has been derived from high-level quantum chemical calculations. The most favorable pathways for the reactions of the $[OSiOH]^+/CH_4$ couple were located on the singlet potential energy surface (PES) as shown in Figure 2. An encounter complex **1** is initially formed from the reactants; this barrier-free step is exothermic by 104 kJ mol^{-1}, thus indicating a rather strong interaction between the positively charged silicon atom and methane (the charge on the silicon atom of $[OSiOH]^+$ amounts to 2.5|e| based on a natural bond orbital (NBO) analysis). Subsequently, one C—H bond of the incoming hydrocarbon substrate is activated and a hydrogen atom is transferred to the oxo-group of $[OSiOH]^+$ via transition state **TS1/2** to form the rather stable silyl cation **2**. In the latter, the positive charge at the silicon atom amounts to 2.41|e|, and the formations of strong Si—C and O—H bonds account for the high stability of **2**; the calculated homolytic Si—C bond energy in **2** is 428 kJ mol^{-1}, close to the reported value of silicon carbide.[21] Next, rather than homolytically splitting the Si—C bond of **2**, the methyl group can migrate via **TS2/3** to one of the hy-
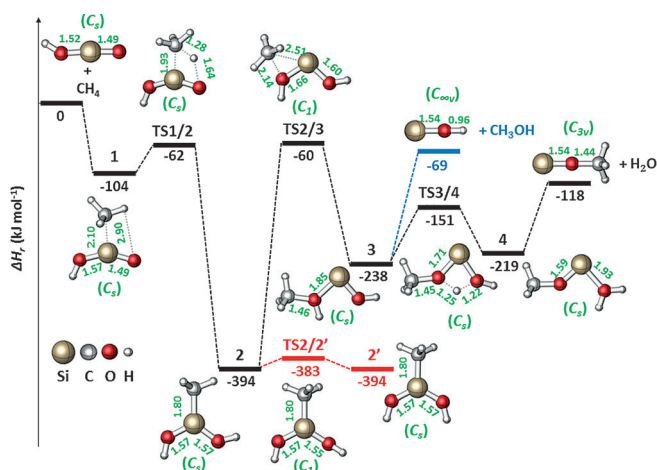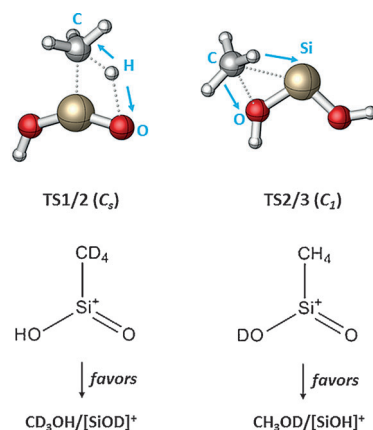
⇗⇖ These are not the final page numbers!

Figure 2. PES and selected structural information of the associated species for the reaction of singlet [OSiOH]$^+$ with CH_4 at the CCSD(T)/C//BMK/B level of theory. Zero-point corrected relative energies are given in kJ mol^{-1} and bond lengths in Å; charges are omitted for the sake of clarity.

droxide ligands, thus forming complex **3**. This intermediate then serves as a branching point to liberate either CH_3OH with the formation of [SiOH]$^+$ or to bring about H_2O loss accompanied by the generation of [SiOCH$_3$]$^+$. For the latter route, complex **3** first isomerizes to intermediate **4** via **TS3/4**. As this step and the elimination of H_2O to produce [SiOCH$_3$]$^+$ are much less energy-demanding than the formation of [SiOH]$^+$ and CH_3OH, a higher branching ratio in favor of [SiOCH$_3$]$^+$ is expected, in line with the experimental findings. In the overall activation of CH_4 by [OSiOH]$^+$, the energetically most demanding steps correspond to the transition states **TS1/2** and **TS2/3**; however, as both are located approximately 60 kJ mol^{-1} below the entrance channel, in line with the experimental results, facile activation of CH_4 can occur under ambient conditions.

For the formation of [SiOH]$^+$ and, in particular, the generation of [SiOH]$^+$ and [SiOD]$^+$ from the [OSiOH]$^+$/CD$_4$ couple (Figure 1 c), the PES analysis is quite instructive. Since the rotation around the Si—O bond in **2** is energetically extremely favorable, the two hydroxide ligands become constitutionally equivalent (as shown for **2** $\rightleftarrows$ **TS2/2'** $\rightleftarrows$ **2'**). Thus, the formations of [SiOH]$^+$ and [SiOD]$^+$ from [OSiOH]$^+$/CD$_4$ are expected to occur because the rebound of the CD$_3$ group can involve either the -OH or the -OD unit. However, in the absence of a significant secondary KIE, which can only be expected when the hybridization in the reaction center is changed in the TS compared to the adduct[22] (and this is not the case for reaction step **2**→**3**), the experimentally observed ratio [SiOH]$^+$:[SiOD]$^+$ of 1:1.8 is not compatible with this reasoning since a 1:1 ratio is expected under the assumptions that 1) both hydroxy groups are indistinguishable, 2) the intramolecular energy redistribution of the rovibrationally hot intermediates **2** and **3** is complete (ergodic behavior[23]), and 3) dynamic effects do not matter.[24] Thus, other processes must be taken into account that explain the preferred formation of [SiOD]$^+$ from the [OSiOH]$^+$/CD$_4$ couple. Since the barrier **TS1/2** is lower than **TS2/3**,[25] an H/D scrambling process along **1**$\rightleftarrows$**2** is possible. As a consequence, the H/D exchange of the deuterated methyl group with the hydrox-

ide ligand OH in [(OH)Si(CD$_3$)(OD)]$^+$ leads to the formation of the complex [(OD)Si(CD$_2$H)(OD)]$^+$; thus, more [SiOD]$^+$ is formed under the liberation of CD$_2$HOD. The existence of an H/D exchange is indeed confirmed also in the reaction of the [OSiOD]$^+$/CH$_4$ couple (Figure 1 e). After hydrogen abstraction by the oxo group of [OSiOD]$^+$ forming the complex [(OH)Si(-CH$_3$)(OD)]$^+$, H/D exchange gives rise to the complex [(OH)-Si(CH$_2$D)(OH)]$^+$; as a consequence, more [SiOH]$^+$ is formed along with the liberation of CH$_2$DOH. The fact that an H/D exchange through **2**$\rightleftarrows$**3** occurs is further substantiated by the signals for [SiOCHD$_2$]$^+$ and [SiOCH$_2$D]$^+$ in Figures 1 c and 1 e, respectively. However, the intensity of these two signals is rather small compared to the signals for the generation of [SiOCD$_3$]$^+$ and [SiOCH$_3$]$^+$from [OSiOH]$^+$/CD$_4$ and [OSiOD]$^+$/CH$_4$, respectively. As a consequence, the H/D exchange alone is not likely to explain the [SiOH]$^+$/[SiOD]$^+$ ratios given in Figures 1 c, d, and e. It is possible to speculate that the rovibrationally active **TS1/2** and **TS2/3** are also subject to dynamic effects as indicated by the vectors for the movement of the incipient methyl group in each case (Scheme 1). Accordingly, we expect the production of more [SiOD]$^+$ and [SiOH]$^+$ from [OSiOH]$^+$/CD$_4$ and [OSiOD]$^+$/CH$_4$ couple, respectively, in line with the experimental findings. Clearly, a much more detailed analysis would be required to describe the branching ratios in a quantitative manner. However, this is beyond our present capabilities.

Scheme 1. Dynamic effects indicated by the vectors for the movement of the incipient methyl group in **TS1/2** and **TS2/3**.

To achieve a more thorough understanding of the reactivity of [OSiOH]$^+$ towards CH_4, we have also investigated the related open-shell system [SiO$_2$]$^+$/CH$_4$. Whereas [SiO$_2$]$^+$ reacts with H_2O to generate [SiO$_2$H]$^+$, it is not capable to bring about C—H bond activation of methane. The difference in reactivity, favoring activation of the strong O—H bond of water, can be ascribed to different reaction mechanisms, as reported previously.[26] The inertness of [SiO$_2$]$^+$ towards CH_4 can be well explained by quantum chemical calculations (Figure 3). Instead of having a terminal oxyl radical, possessing a high spin density, the most stable structure of [SiO$_2$]$^+$ in its doublet ground state corresponds to a superoxide configuration, in which the two oxygen atoms are bridged by a cationic silicon atom. The

O—O bond length of $[SiO_2]^+$ amounts to 1.34 Å and is thus similar to that of free O_2^- (1.33 Å);[27] the spin is evenly distributed over the two oxygen atoms (0.53 for each). This structure is about 18 kJ mol^{-1} lower in energy than the linear $[OSiO]^+$ isomer. Furthermore, only Si$^+$ (m/z:28) is observed in a collisional activation experiment of $[SiO_2]^+$, supporting the presence of an O—O bond in this cluster. According to the PES shown in Figure 3, due to an intact O—O bond and lacking an oxygen-centered radical, the reaction with methane is kinetically hindered by a barrier of 28 kJ mol^{-1} relative to the entrance channel, and therefore not accessible at ambient conditions. Regarding the previously studied $[SiO]^+/CH_4$ couple,[28] in this system the spin density is exclusively located at the oxygen atom, thus representing a 'prepared' state.[5d] Consequently, $[SiO]^+$ brings about efficient activation of methane at room temperature. However, in contrast to the closed-shell couple $[OSiOH]^+/CH_4$, which gives rise to the generation of closed-shell molecules, for example, CH_3OH and H_2O, a CH_3-radical is generated in the open-shell system $[SiO]^+/CH_4$. Evidently, the chemoselectivity of methane activation can be controlled by switching between open- and closed-shell oxide cluster ions.
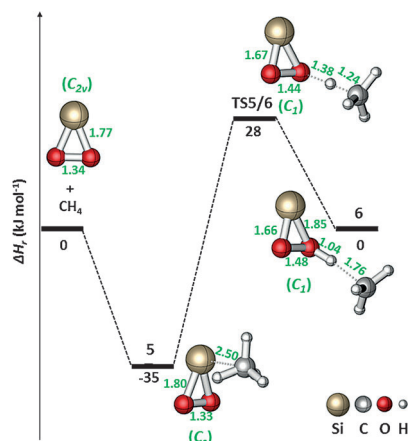
CH_4 reveals that the energy gained in generating an encounter complex **7** amounts to only 11 kJ mol^{-1}; this is not sufficient to energetically pull down transition state **TS7/8** below the entrance channel. Based on an NBO analysis, the charge on the carbon atom of $[OCOH]^+$ amounts to $1.2|e|$, which is much less than that of the silicon atom in $[OSiOH]^+$ ($2.5|e|$), that is, in the silicon system, the higher Lewis acidity results in a much stronger interaction of the oxide cluster ion with the incoming hydrocarbon substrate. Moreover, the absolute HAT barrier height for the cleavage of the strong C=O bond in $[OCOH]^+$ (**TS7/8**, 81 kJ mol^{-1}) is much higher when compared to that of **TS1/2** (42 kJ mol^{-1}). Thus, while the production of $[CH_3CO]^+/H_2O$ is exothermic, the reaction is kinetically hindered, and, in line with the experimental findings, does not take place. Another pathway for the reaction of $[OCOH]^+$ with CH_4 corresponds to the well-known proton transfer to form $[CH_5]^+$; this process is exothermic by 2 kJ mol^{-1}, in line with the experimental data of the proton affinities (PA(CH_4) = 543.5 kJ mol^{-1} and PA(CO_2) = 540.5 kJ mol^{-1}).[30]

Figure 3. PES and key ground-state structures involved in the reactions of doublet $[SiO_2]^+$ with CH_4 at the CCSD(T)/C//BMK/B level of theory. Zero-point corrected relative energies are given in kJ mol^{-1} and bond lengths in Å; charges are omitted for the sake of clarity.
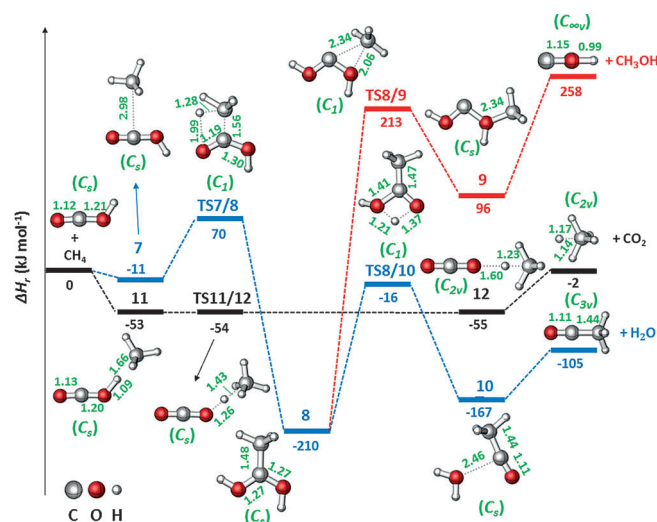

Figure 4. PES and selected structural information of the associated species for the reactions of singlet $[OCOH]^+$ with CH_4 at the CCSD(T)/C//BMK/B level of theory. Zero-point corrected relative energies are given in kJ mol^{-1} and bond lengths in Å; charges are omitted for the sake of clarity. Note that the energy of intermediate **11** is a little higher than the transition state **TS11/12** due to zero-point energy correction.

A comparison of $[OSiOH]^+$ with other closed-shell species is also instructive as this may address the question, what are the prominent features of $[OSiOH]^+$ that cause its quite distinctive reactivity towards methane? Thus, in order to obtain further insight into the C—H bond activation by closed-shell clusters, we have also computationally addressed the reactivity of $[OCOH]^+$ and $[MgOH]^+$ towards CH_4. The latter is closely related to the open-shell cluster $[MgO]^+$, which has been extensively studied both in the condensed and in the gas phase for methane activation.[29]

Regarding the $[OCOH]^+/CH_4$ couple, according to the calculations, only the generation of $[CH_3CO]^+$ upon water elimination is exothermic (Figure 4). However, in contrast to the $[OSiOH]^+/CH_4$ system, in which CH_4 is strongly bound to the silicon atom in the encounter complex **1**, the PES of $[OCOH]^+/$

The reaction of $[MgOH]^+$ with CH_4 is shown in Figure 5. For the singlet PES, it commences by forming stable encounter complex **13**, in which CH_4 is coordinated at a vacant site of the Mg atom of $[MgOH]^+$. Although this interaction is quite strong (93 kJ mol^{-1}), the subsequent intra-complex H transfer from CH_4 to the oxygen atom of the hydroxyl group of $[MgOH]^+$ encounters a significant kinetic barrier, which amounts to 27 kJ mol^{-1} relative to the reactants, and can therefore not be surmounted under ambient conditions. Furthermore, a comparison of the absolute barriers for H transfer from CH_4 to the hydroxo groups of $[MgOH]^+$ and $[OSiOH]^+$, reveals that this step is more energy demanding for the former system (i.e., 120 kJ mol^{-1} for $[MgOH]^+/CH_4$ versus 88 kJ mol^{-1} for $[OSiOH]^+/$

↖↖ **These are not the final page numbers!**

CH_4). Moreover, whereas the silyl cation intermediate [(OH)Si(-CH_3)(OH)]$^+$ (**2**, Figure 2) is much lower in energy compared to the encounter complex [(OH)Si(CH_4)(O)]$^+$ (**1**), the isomers **13** and **14** (Figure 5) are almost of equal energy. The reason for this is that the processes for bond breaking and bond making of the steps **1**→**2** and **13**→**14** (Figures 2 and 5, respectively) are much more favorable for the silicon system compared to the magnesium species. Thus, according to the calculations, the newly formed Si–C bond is much stronger than the Mg–C bond (428 kJ mol^{-1} compared to 232 kJ mol^{-1}, respectively). Whereas the hydrogen transfer in the [OSiOH]$^+$/CH_4 system involves the cleavage of a relatively weak Si=O π-bond, a quite substantial effort is required for weakening of the Mg–O bond in the [MgOH]$^+$/CH_4 couple (the Si–O bond lengths amount to 1.49 Å and 1.57 Å in intermediates **1** and **2**, respectively, Figure 2. Also, the Mg–O bond is elongated from 1.71 Å in **13** to 2.00 Å in **14**, Figure 5). Furthermore, the H transfer from methane to the hydroxo ligand of [OSiOH]$^+$ is 46 kJ mol^{-1} less favorable than the H transfer to the oxo group of this cluster; this option does not exist for [MgOH]$^+$.
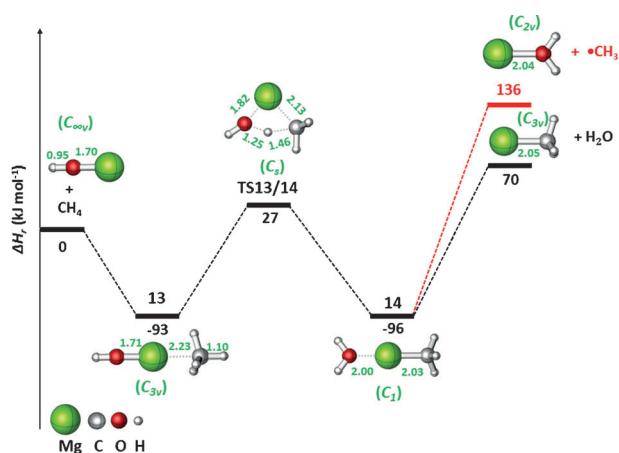

Figure 5. PES and selected structural information of the associated species for the reaction of singlet [MgOH]$^+$ with CH_4 at the CCSD(T)/C//BMK/B level of theory. Zero-point corrected, relative energies are given in kJ mol^{-1} and bond lengths in Å; charges are omitted for the sake of clarity.

Conclusion

In summary, our experimental and theoretical studies demonstrate that the closed-shell cluster ion [OSiOH]$^+$ efficiently activates methane, giving rise to [SiOH]$^+$ and [SiOCH$_3$]$^+$ upon elimination of the neutral closed-shell products CH_3OH and H_2O, respectively. By comparing the [OSiOH]$^+$/CH_4 couple with those of the closed-shell systems [OCOH]$^+$/CH_4 and [MgOH]$^+$/CH_4, the capability of [OSiOH]$^+$ to thermally activate methane can be traced back to the higher Lewis acidity of the silicon atom in [OSiOH]$^+$ versus that of the carbon atom in [OCOH]$^+$, resulting in a stronger interaction with methane that favors hydrogen-atom transfer to the oxo group. The absolute barrier of this step further benefits from the cleavage of the relatively weak Si=O bond, whereas the weakening of the strong ionic

Mg–OH interaction disfavors the H transfer to the OH group in the [MgOH]$^+$/CH_4 system.

To the best of our knowledge, this is the first example of a hydrogen-atom transfer in a closed-shell, metal-free cluster. These results not only deepen our mechanistic understanding of C–H bond activation, but may also shed light on the role of silicon oxide surfaces in heterogeneous catalysis, underlining its potential as a possible metal-free catalyst.

Experimental and Computational Details

The experiments were carried out using a Spectrospin-CMS-47X Fourier-transform ion cyclotron resonance (FT-ICR) mass spectrometer as described elsewhere.[31] In brief, [SiO$_2$]$^+$ cations were generated by laser ablation of a rotating silicon plate using a Nd:YAG laser ($\lambda = 1064$ nm) in the presence of about 1% O$_2$ seeded in helium carrier gas. The [SiO$_2$]$^+$ ions were transferred from the external ion source into the cylindrical ICR cell, which is positioned in a superconducting magnet field (7.05 T), by using a system of electrostatic potentials and lenses. [OSiOH]$^+$ was generated by the reaction of [SiO$_2$]$^+$ with background water in the ICR cell. Thermalization of the ions of interest has been achieved by collisions with repeatedly pulsed-in argon. Collisional activation experiments[32] were performed for structural investigations through the introduction of argon into the ICR cell for collisions with the ions of interest.

The theoretical work was performed using the Gaussian 09 program.[33] The BMK (Boese-Martin for kinetics) density functional[34] in conjunction with a 6-31+G(2df,p) basis set (BMK/B) were applied to optimize the structures of stationary points along the reaction coordinates; this level of theory has previously been proven to be able to reproduce experimental results for C–H bond activation processes with rather small error bars;[35] the single-point energies of optimized structures have been recalculated by using CCSD(T)[36] with the aug-cc-pVTZ basis set (CCSD(T)/C). Stationary points were optimized without symmetry constraint, and their nature confirmed by vibrational frequency analysis. Intrinsic reaction coordinate[37] calculations were performed to link transition structures with the respective intermediates. Unscaled vibrational frequencies were used to correct the relative energies for zero-point energy (ZPE) contributions. All the optimized Cartesian coordinates as well as computed total energies and ZPE energies have been given in the supporting information.

[1] a) G. A. Olah, A. Goeppert, G. K. S. Prakash, *Beyond Oil and Gas: The Methanol Economy*, Wiley-VCH, Weinheim, **2009**; b) J. R. Webb, T. Bolano, T. B. Gunnoe, *ChemSusChem* **2011**, *4*, 37–49; c) R. Horn, R. Schlögl, *Catal. Lett.* **2015**, *145*, 23–39.

[2] a) F. Arena, A. Parmaliana, *Acc. Chem. Res.* **2003**, *36*, 867–875; b) C. Coperet, *Chem. Rev.* **2010**, *110*, 656–680; c) Z. Guo, B. Liu, Q. H. Zhang, W. P. Deng, Y. Wang, Y. H. Yang, *Chem. Soc. Rev.* **2014**, *43*, 3480–3524; d) R. Schlögl, *Angew. Chem. Int. Ed.* **2015**, *54*, 3465–3520; *Angew. Chem.* **2015**, *127*, 3531–3589.

[3] a) D. Schröder, H. Schwarz, *Angew. Chem. Int. Ed. Engl.* **1995**, *34*, 1973–1995; *Angew. Chem.* **1995**, *107*, 2126–2150; b) D. K. Bohme, H. Schwarz, *Angew. Chem. Int. Ed.* **2005**, *44*, 2336–2354; *Angew. Chem.* **2005**, *117*, 2388–2406; c) J. Roithova, D. Schröder, *Chem. Rev.* **2010**, *110*, 1170–1211; d) H. Schwarz, *Angew. Chem. Int. Ed.* **2011**, *50*, 10096–10115; *Angew. Chem.* **2011**, *123*, 10276–10297; e) S. M. Lang, T. M. Bernhardt, *Phys. Chem. Chem. Phys.* **2012**, *14*, 9255–9269; f) D. J. Harding, A. Fielicke, *Chem. Eur. J.* **2014**, *20*, 3258–3267.

[4] For an exhaustive review, see: H. Schwarz, *Chem. Phys. Lett.* **2015**, *629*, 91–101.

[5] For reviews, see: a) Y. X. Zhao, X. L. Ding, Y. P. Ma, Z. C. Wang, S. G. He, *Theor. Chem. Acc.* **2010**, *127*, 449–465; b) N. Dietl, M. Schlangen, H. Schwarz, *Angew. Chem. Int. Ed.* **2012**, *51*, 5544–5555; *Angew. Chem.* **2012**, *124*, 5638–5650; c) X. L. Ding, X. N. Wu, Y. X. Zhao, S. G. He, *Acc. Chem. Res.* **2012**, *45*, 382–390; d) W. Z. Lai, C. S. Li, H. Chen, S. Shaik, *Angew. Chem. Int. Ed.* **2012**, *51*, 5556–5578; *Angew. Chem.* **2012**, *124*, 5652–5676; e) H. Schwarz, *Isr. J. Chem.* **2014**, *54*, 1413–1431.

[6] a) D. Schröder, H. Schwarz, *Angew. Chem. Int. Ed. Engl.* **1990**, *29*, 1433–1434; *Angew. Chem.* **1990**, *102*, 1468–1469; b) G. Altinay, M. Citir, R. B. Metz, *J. Phys. Chem. A* **2010**, *114*, 5104–5112; c) N. Dietl, C. van der Linde, M. Schlangen, M. K. Beyer, H. Schwarz, *Angew. Chem. Int. Ed.* **2011**, *50*, 4966–4969; *Angew. Chem.* **2011**, *123*, 5068–5072; d) S. D. Zhou, J. L. Li, M. Schlangen, H. Schwarz, *Angew. Chem. Int. Ed.* **2016**, DOI: 10.1002/anie.201605259 and 10.1002/ange.201605259.

[7] a) P. B. Armentrout, *Science* **1991**, *251*, 175–179; b) S. Shaik, M. Filatov, D. Schröder, H. Schwarz, *Chem. Eur. J.* **1998**, *4*, 193–199; c) D. Schröder, S. Shaik, H. Schwarz, *Acc. Chem. Res.* **2000**, *33*, 139–145; d) S. Shaik, S. P. de Visser, F. Ogliaro, H. Schwarz, D. Schröder, *Curr. Opin. Chem. Biol.* **2002**, *6*, 556–567; e) H. Schwarz, *Int. J. Mass Spectrom.* **2004**, *237*, 75–105; f) S. Shaik, D. Kumar, S. P. de Visser, A. Altun, W. Thiel, *Chem. Rev.* **2005**, *105*, 2279–2328; g) P. E. M. Siegbahn, T. Borowski, *Acc. Chem. Res.* **2006**, *39*, 729–738; h) W. Nam, *Acc. Chem. Res.* **2007**, *40*, 522–531; i) S. Shaik, H. Hirao, D. Kumar, *Acc. Chem. Res.* **2007**, *40*, 532–542; j) S. Shaik, *Int. J. Mass Spectrom.* **2013**, *354*, 5–14; k) J. N. Harvey, *WIREs Comput. Mol. Sci.* **2014**, *4*, 1–14.

[8] For a review, see: H. Schwarz, *Angew. Chem. Int. Ed.* **2003**, *42*, 4442–4454; *Angew. Chem.* **2003**, *115*, 4580–4593.

[9] For a recent review, see: S. D. Zhou, J. L. Li, M. Schlangen, H. Schwarz, *Acc. Chem. Res.* **2016**, *49*, 494–502.

[10] a) K. K. Irikura, J. L. Beauchamp, *J. Am. Chem. Soc.* **1989**, *111*, 75–85; b) M. Pavlov, M. R. A. Blomberg, P. E. M. Siegbahn, R. Wesendrup, C. Heinemann, H. Schwarz, *J. Phys. Chem. A* **1997**, *101*, 1567–1579; c) G. B. Zhang, S. H. Li, Y. S. Jiang, *Organometallics* **2004**, *23*, 3656–3667; d) A. Bozovic, S. Feil, G. K. Koyanagi, A. A. Viggiano, X. H. Zhang, M. Schlangen, H. Schwarz, D. K. Bohme, *Chem. Eur. J.* **2010**, *16*, 11605–11610.

[11] R. Kretschmer, M. Schlangen, H. Schwarz, *Angew. Chem. Int. Ed.* **2013**, *52*, 6097–6101; *Angew. Chem.* **2013**, *125*, 6213–6217.

[12] S. D. Zhou, J. L. Li, M. Schlangen, H. Schwarz, *Chem. Eur. J.* **2016**, DOI: 10.1002/chem.201600498.

[13] S. D. Zhou, J. L. Li, M. Schlangen, H. Schwarz, *Angew. Chem. Int. Ed.* **2016**, DOI: 10.1002/anie201602312.

[14] a) T. Y. Cheng, Q. K. Zhao, D. C. Zhang, G. H. Liu, *Green Chem.* **2015**, *17*, 2100–2122; b) S. Soled, *Science* **2015**, *350*, 1171–1172; c) L. B. Sun, X. Q. Liu, H. C. Zhou, *Chem. Soc. Rev.* **2015**, *44*, 5092–5147.

[15] The entire issue is dedicated to this topic: *Appl. Catal. A* **1997**, *157*, 1–425 .

[16] L. D. Nguyen, S. Loridant, H. Launay, A. Pigamo, J. L. Dubois, J. M. M. Millet, *J. Catal.* **2006**, *237*, 38–48.

[17] X. G. Guo, G. Z. Fang, G. Li, H. Ma, H. J. Fan, L. Yu, C. Ma, X. Wu, D. H. Deng, M. M. Wei, D. L. Tan, R. Si, S. Zhang, J. Q. Li, L. T. Sun, Z. C. Tang, X. L. Pan, X. H. Bao, *Science* **2014**, *344*, 616–619.

[18] a) J. Zhang, X. Liu, R. Blume, A. H. Zhang, R. Schlögl, D. S. Su, *Science* **2008**, *322*, 73–77; b) G. de Petris, A. Troiani, M. Rosi, G. Angelini, O. Ursini, *Chem. Eur. J.* **2009**, *15*, 4248–4252; c) N. Dietl, M. Engeser, H. Schwarz, *Angew. Chem. Int. Ed.* **2009**, *48*, 4861–4863; *Angew. Chem.*

[2009], *121*, 4955–4957; d) M. A. Legare, M. A. Courtemanche, E. Rochette, F. G. Fontaine, *Science* **2015**, *349*, 513–516.

[19] M. T. Bowers, J. B. Laudenslager, *J. Chem. Phys.* **1972**, *56*, 4711–4712.

[20] D. Schröder, H. Schwarz, D. E. Clemmer, Y. M. Chen, P. B. Armentrout, V. I. Baranov, D. K. Bohme, *Int. J. Mass Spectrom.* **1997**, *161*, 175–191.

[21] Y. R. Luo, *Comprehensive Handbook of Chemical Bond Energies*, CRC, Boca Raton, **2007**.

[22] E. V. Anslyn, D. A. Dougherty, *Modern Physical Organic Chemistry*, University Science Books, Sausalito, **2006**.

[23] For reviews as well as examples of a non-ergodic behavior, see: a) I. Oref, B. S. Rabinovitch, *Acc. Chem. Res.* **1979**, *12*, 166–175; b) G. Depke, C. Lifshitz, H. Schwarz, E. Tzidony, *Angew. Chem. Int. Ed. Engl.* **1981**, *20*, 792–793; *Angew. Chem.* **1981**, *93*, 824–825; c) C. Lifshitz, *J. Phys. Chem.* **1983**, *87*, 2304–2313; d) B. K. Carpenter, *Acc. Chem. Res.* **1992**, *25*, 520–528; e) B. K. Carpenter, *Annu. Rev. Phys. Chem.* **2005**, *56*, 57–89; f) U. Lourderaj, K. Park, W. L. Hase, *Int. Rev. Phys. Chem.* **2008**, *27*, 361–403; g) H. Yamataka, M. Sato, H. Hasegawa, S. C. Ammal, *Faraday Discuss.* **2010**, *145*, 327–340; h) R. P. Pemberton, Y. J. Hong, D. J. Tantillo, *Pure Appl. Chem.* **2013**, *85*, 1949–1957; i) Z. Y. Yang, C. Doubleday, K. N. Houk, *J. Chem. Theory Comput.* **2015**, *11*, 5606–5612.

[24] For a recent perspective article on this topic, see: a) B. K. Carpenter, J. N. Harvey, A. J. Orr-Ewing, *J. Am. Chem. Soc.* **2016**, *138*, 4695–4705, and numerous references therein; b) W. L. Hase, *Science* **1994**, *266*, 998–1002.

[25] Note that the relative energies of **TS1/2** versus **TS2/3** are affected by the theoretical method employed for making the zero-point energy corrections; but they are always in favor of **TS1/2**. For example, using the G4 method, **TS1/2** is $22\,\mathrm{kJ\,mol^{-1}}$ lower in energy than **TS2/3**.

[26] a) J. L. Li, S. D. Zhou, X. N. Wu, S. Y. Tang, M. Schlangen, H. Schwarz, *Angew. Chem. Int. Ed.* **2015**, *54*, 11861–11864; *Angew. Chem.* **2015**, *127*, 12028–12032; b) J. L. Li, X. N. Wu, S. D. Zhou, S. Y. Tang, M. Schlangen, H. Schwarz, *Angew. Chem. Int. Ed.* **2015**, *54*, 12298–12302; *Angew. Chem.* **2015**, *127*, 12472–12477.

[27] D. R. Lide, *Handbook of Chemistry and Physics*, CRC, Taylor and Francis, 90th ed., **2009**.

[28] N. Dietl, A. Troiani, M. Schlangen, O. Ursini, G. Angelini, Y. Apeloig, G. de Petris, H. Schwarz, *Chem. Eur. J.* **2013**, *19*, 6662–6669.

[29] a) R. H. Nibbelke, J. Scheerova, M. H. J. M. Decroon, G. B. Marin, *J. Catal.* **1995**, *156*, 106–119; b) C. W. Hu, H. Q. Yang, N. B. Wong, Y. Q. Chen, M. C. Gong, A. M. Tian, C. Li, W. K. Li, *J. Phys. Chem. A* **2003**, *107*, 2316–2323; c) D. Schröder, J. Roithova, *Angew. Chem. Int. Ed.* **2006**, *45*, 5705–5708; *Angew. Chem.* **2006**, *118*, 5835–5838; d) K. Kwapien, M. Sierka, J. Döbler, J. Sauer, *ChemCatChem* **2010**, *2*, 819–826; e) P. Myrach, N. Nilius, S. V. Levchenko, A. Gonchar, T. Risse, K. P. Dinse, L. A. Boatner, W. Frandsen, R. Horn, H. J. Freund, R. Schlögl, M. Scheffler, *ChemCatChem* **2010**, *2*, 854–862; f) S. Arndt, G. Laugel, S. Levchenko, R. Horn, M. Baerns, M. Scheffler, R. Schlögl, R. Schomacker, *Catal. Rev. Sci. Eng.* **2011**, *53*, 424–514; g) K. Kwapien, M. Sierka, J. Dobler, J. Sauer, M. Haertelt, A. Fielicke, G. Meijer, *Angew. Chem. Int. Ed.* **2011**, *50*, 1716–1719; *Angew. Chem.* **2011**, *123*, 1754–1757; h) P. Schwach, M. G. Willinger, A. Trunschke, R. Schlögl, *Angew. Chem. Int. Ed.* **2013**, *52*, 11381–11384; *Angew. Chem.* **2013**, *125*, 11591–11594; i) K. Kwapien, J. Paier, J. Sauer, M. Geske, U. Zavyalova, R. Horn, P. Schwach, A. Trunschke, R. Schlögl, *Angew. Chem. Int. Ed.* **2014**, *53*, 8774–8778; *Angew. Chem.* **2014**, *126*, 8919–8923.

[30] a) G. G. Meisels, R. K. Mitchum, J. P. Freeman, *J. Phys. Chem.* **1976**, *80*, 2845–2848; b) E. P. L. Hunter, S. G. Lias, *J. Phys. Chem. Ref. Data* **1998**, *27*, 413–656.

[31] a) K. Eller, H. Schwarz, *Int. J. Mass Spectrom. Ion Processes* **1989**, *93*, 243–257; b) K. Eller, W. Zummack, H. Schwarz, *J. Am. Chem. Soc.* **1990**, *112*, 621–627; c) M. Engeser, T. Weiske, D. Schröder, H. Schwarz, *J. Phys. Chem. A* **2003**, *107*, 2855–2859.

[32] K. Levsen, H. Schwarz, *Mass Spectrom. Rev.* **1983**, *2*, 77–148.

[33] Gaussian 09, Revision A.02, M. J. Frisch, G. W. Trucks, H. B. Schlegel, G. E. Scuseria, M. A. Robb, J. R. Cheeseman, G. Scalmani, V. Barone, B. Mennucci, G. A. Petersson, H. Nakatsuji, M. Caricato, X. Li, H. P. Hratchian, A. F. Izmaylov, J. Bloino, G. Zheng, J. L. Sonnenberg, M. Hada, M. Ehara, K. Toyota, R. Fukuda, J. Hasegawa, M. Ishida, T. Nakajima, Y. Honda, O. Kitao, H. Nakai, T. Vreven, J. A. Montgomery, Jr., J. E. Peralta, F. Ogliaro, M. Bearpark, J. J. Heyd, E. Brothers, K. N. Kudin, V. N. Staroverov, R. Kobayashi, J. Normand, K. Raghavachari, A. Rendell, J. C. Burant, S. S. Iyen-

gar, J. Tomasi, M. Cossi, N. Rega, J. M. Millam, M. Klene, J. E. Knox, J. B. Cross, V. Bakken, C. Adamo, J. Jaramillo, R. Gomperts, R. E. Stratmann, O. Yazyev, A. J. Austin, R. Cammi, C. Pomelli, J. W. Ochterski, R. L. Martin, K. Morokuma, V. G. Zakrzewski, G. A. Voth, P. Salvador, J. J. Dannenberg, S. Dapprich, A. D. Daniels, Ö. Farkas, J. B. Foresman, J. V. Ortiz, J. Cioslowski, D. J. Fox, Gaussian, Inc. Wallingford CT, 2009..

[34] A. D. Boese, J. M. L. Martin, *J. Chem. Phys.* **2004**, *121*, 3405–3416.

[35] a) R. P. Huo, X. A. Zhang, X. R. Huang, J. L. Li, C. C. Sun, *J. Phys. Chem. A* **2011**, *115*, 3576–3582; b) N. Li, R. P. Huo, X. A. Zhang, X. R. Huang, J. L. Li, C. C. Sun, *Chem. Phys. Lett.* **2011**, *503*, 210–214; c) R. P. Huo, X. R. Huang, J. L. Li, X. Zhang, N. Li, C. C. Sun, *Int. J. Quantum Chem.* **2012**, *112*, 1078–1085; d) X. Z. R. P. Huo, X. R. Huang, J. L. Li, C. C. Sun, *Acta Chim. Sin.* **2013**, *71*, 743–748.

[36] a) G. D. Purvis, R. J. Bartlett, *J. Chem. Phys.* **1982**, *76*, 1910–1918; b) J. A. Pople, M. Headgordon, K. Raghavachari, *J. Chem. Phys.* **1987**, *87*, 5968–5975; c) G. E. Scuseria, C. L. Janssen, H. F. Schaefer, *J. Chem. Phys.* **1988**, *89*, 7382–7387.

[37] a) K. Fukui, *Acc. Chem. Res.* **1981**, *14*, 363–368; b) D. G. Truhlar, N. J. Kilpatrick, B. C. Garrett, *J. Chem. Phys.* **1983**, *78*, 2438–2442; c) H. P. Hratchian, H. B. Schlegel, *J. Chem. Theory Comput.* **2005**, *1*, 61–69.
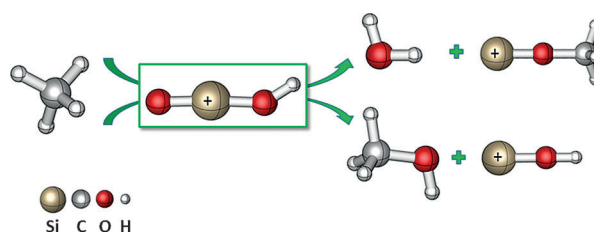
These are not the final page numbers! ↗↗

FULL PAPER

X. Sun, S. Zhou, M. Schlangen,
H. Schwarz*

■■ – ■■

Efficient Room-Temperature Methane Activation by the Closed-Shell, Metal-Free Cluster [OSiOH]+: A Novel Mechanistic Variant

Si C O H

The closed-shell cluster ion [OSiOH]+ can efficiently mediate C–H bond activation at room temperature, giving rise to [SiOH]+ and [SiOCH3]+ under the concomitant formation of methanol and water, respectively. Mechanistic aspects for this unprecedented reactivity pattern are presented.

↖↖ These are not the final page numbers!